



HAL
open science

High precision scale setting on the lattice

Sz. Borsanyi, Z. Fodor, J. Guenther, C. Hoelbling, S. Katz, Laurent Lellouch,
T. Lippert, K. Miura, L. Parato, K. Szabo, et al.

► **To cite this version:**

Sz. Borsanyi, Z. Fodor, J. Guenther, C. Hoelbling, S. Katz, et al.. High precision scale setting on the lattice. The 38th International Symposium on Lattice Field Theory, Jul 2021, Zoom/Gather@Massachusetts Institute of Technology, United States. pp.371, 10.22323/1.396.0371 . hal-03870831

HAL Id: hal-03870831

<https://hal.science/hal-03870831v1>

Submitted on 28 Nov 2022

HAL is a multi-disciplinary open access archive for the deposit and dissemination of scientific research documents, whether they are published or not. The documents may come from teaching and research institutions in France or abroad, or from public or private research centers.

L'archive ouverte pluridisciplinaire **HAL**, est destinée au dépôt et à la diffusion de documents scientifiques de niveau recherche, publiés ou non, émanant des établissements d'enseignement et de recherche français ou étrangers, des laboratoires publics ou privés.

High precision scale setting on the lattice

**Sz. Borsanyi,^a Z. Fodor,^{a,b,c,d,e} J. N. Guenther,^{a,f} C. Hoelbling,^a S. D. Katz,^d
L. Lellouch,^f T. Lippert,^{a,b} K. Miura,^{f,g,h} L. Parato,^f K. K. Szabo,^{a,b} F. Stokes,^b
B. C. Toth,^a Cs. Torok^b and L. Varnhorst^{a,f,*}**

^aDepartment of Physics, University of Wuppertal, D-42119 Wuppertal, Germany

^bJülich Supercomputing Centre, Forschungszentrum Jülich, D-52428 Jülich, Germany

^cDepartment of Physics, Pennsylvania State University, University Park, PA 16802, USA

^dInstitute for Theoretical Physics, Eötvös University, H-1117 Budapest, Hungary

^eUniversity of California, San Diego, 9500 Gilman Drive, La Jolla, CA 92093, USA

^fAix Marseille Univ., Université de Toulon, CNRS, CPT, IPhU, Marseille, France

^gHelmholtz Institute Mainz, D-55099 Mainz, Germany

^hKobayashi-Maskawa Institute for the Origin of Particles and the Universe, Nagoya University, Nagoya 464-8602, Japan

E-mail: varnhorst@uni-wuppertal.de

Recently, the hadronic vacuum polarization contribution to the anomalous magnetic moment of the muon was determined by the BMW collaboration with sub-percent precision. Such a precision requires to control many sources of uncertainty. One of these is the uncertainty in the determination of the lattice spacing. In this talk, we present the scale setting entering this computation. It relies on the mass of the Ω baryon as input which is directly used to set the scale of our main calculation. It also allows us to calculate the value of the intermediate scale setting quantity w_0 . Here, we present our calculation of this quantity with a relative precision of about 0.4%.

*The 38th International Symposium on Lattice Field Theory, LATTICE2021 26th-30th July, 2021
Zoom/Gather@Massachusetts Institute of Technology*

*Speaker

1. Introduction

This work is part of the lattice determination of the anomalous magnetic moment a_μ of the muon by the BMW collaboration that was published in [1]. To achieve the precision necessary for a meaningful comparison with experiments, many sources of errors had to be controlled. One such source is the determination of the lattice scale which is described in this contribution. For an overview of the whole calculation, see also [2]. For our main analysis of a_μ , we set the scale directly with the mass of the omega baryon. To keep this contribution as self contained as possible, however, the determination of w_0 [3] using the omega mass is explained. Besides being a useful quantity by itself, it was also used in [1] to determine the individual isospin splitting contributions to a_μ .

In the first section, the determination of the omega mass on individual ensembles of gauge configurations is discussed, both for the isospin symmetric, pure QCD part as well as for the strong isospin breaking and QED corrections. After that, in a second section, our global fits are briefly explained with a special emphasis on the determination of w_0 .

2. Mass of the omega baryon

Any precise determination of the lattice scale requires a precisely known input quantity. In this work, we choose the mass of the omega baryon. It can be measured both in experiment [4] and on the lattice with sufficient precision.

Our calculation is based on a set of 22 ensembles of gauge configurations generated with a Symanzik improved gauge action. The $2 + 1 + 1$ flavors of the dynamical fermions are realized by a staggered action constructed from four times stout smeared gauge fields. On top of these QCD configuration QED configuration were generated. For details of the action and the methods used to generate the configurations, see [1]. The configurations were generated at six values of the gauge coupling β and the lattice spacing a ranges from 0.132 fm to 0.064 fm. The quark masses were chosen such that the ensembles scatter closely around the physical point to allow for a reliable interpolation to the physical point.

In the first part of this section, the accurate lattice determination of the omega mass in pure QCD is discussed. In the second part, the calculation of the QED corrections, which are important at the target accuracy, is discussed.

2.1 QCD contributions

The mass of the omega baryon can be calculated by studying the exponential falloff of the correlation function of two suitably chosen temporally separated interpolating operators. In the staggered formulation, translations by one lattice spacing are intertwined with transformations among the spinor degrees of freedom of the quark fields. Hence, the construction of interpolating operators that couple to specific hadrons is more complicated than in the case of e.g. Wilson fermions. For mesons, constructions of such operators are discussed in [5]. For the construction of baryon operators, see [6]. Amongst these baryon operators, the ones labeled as VI and XI couple to the omega baryon as the lowest state. The operators can be constructed from a staggered quark

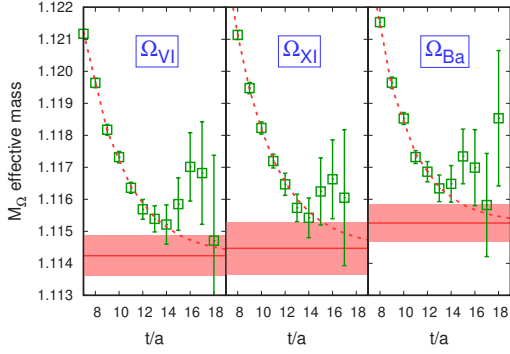


Figure 1: The effective mass of the three operators used for the omega mass determination on the coarsest ensemble. The green data points show the effective masses calculated directly from the correlation function of the respective operators. The red band indicates the ground state mass as extracted with a multistate fit (for details see main text). The red dotted line indicates the effective mass of that multistate fit.

field χ by employing

$$O_{XI}(t) = \sum_{\substack{\vec{x}, x_t=t \\ x_i \text{ even}}} \epsilon^{abc} \left[(D_1\chi^a)(D_{12}\chi^b)(D_{13}\chi^c) - (D_2\chi^a)(D_{21}\chi^b)(D_{23}\chi^c) \right. \\ \left. + (D_3\chi^a)(D_{31}\chi^b)(D_{32}\chi^c) \right], \quad (1a)$$

$$O_{VI}(t) = \sum_{\substack{\vec{x}, x_t=t \\ x_i \text{ even}}} \epsilon^{abc} (D_1\chi^a)(D_2\chi^b)(D_3\chi^c) \quad (1b)$$

where

$$D_i\chi(x) = \frac{1}{2} (\chi(x - \hat{i}) + \chi(x + \hat{i})) \quad \text{and} \quad D_{ij} = D_i D_j. \quad (2)$$

The omega baryon, however, comes in multiple staggered tastes which become degenerate only in the continuum limit. The operators shown above couple to more than one of these tastes. In [7] an additional flavour degree of freedom is used to construct an operator which solely couples to one taste of the omega baryon. This operator reads

$$O_{Ba} = \left[2\delta_{\alpha 1}\delta_{\beta 2}\delta_{\gamma 3} - \delta_{\alpha 3}\delta_{\beta 1}\delta_{\gamma 2} - \delta_{\alpha 2}\delta_{\beta 3}\delta_{\gamma 1} + (\dots \beta \leftrightarrow \gamma \dots) \right] \times \\ \epsilon^{abc} \left((D_1\chi_\alpha^a(x))(D_{12}\chi_\beta^b(x))(D_{13}\chi_\gamma^c(x)) - (D_2\chi_\alpha^a(x))(D_{21}\chi_\beta^b(x))(D_{23}\chi_\gamma^c(x)) + \right. \\ \left. (D_3\chi_\alpha^a(x))(D_{31}\chi_\beta^b(x))(D_{32}\chi_\gamma^c(x)) \right)$$

where the Greek indices refer to the additional flavour degree of freedom. We applied Wuppertal smearing [8], but with a kernel that includes only two-hop terms, to all three operators. For the gauge field appearing in this kernel we applied multiple steps of stout smearing [9] in three dimensions. For details, see [1].

We have compared the performance of the three operators mentioned above on the coarsest ensemble for which we generated about 3000 extra configuration that were used only to compare the three operators with an increased precision. In figure 1 the extracted mass is shown for all three operators. As it can be seen, even on this ensemble the three values agree within errors. Furthermore, the difference between the largest and the smallest value is of the same size than the typical statistical and systematic error on the masses extracted on other ensembles. We conclude that it is therefore justified to use the VI operator to extract the mass of the omega baryon.

Due to the presence of excited states in the correlation functions of the interpolating operators, a simple one-state ansatz does not allow for a controlled extraction of the ground state mass.

Consequently, excited states must be included in the analysis. For this purpose, we employed two procedures: The first one was a fit with a ansatz containing four states. In the second one we used a generalized eigenvalue problem (GEVP) based on a matrix constructed out of time shifted correlation functions [10].

In the first approach, we considered the first four lowest energy states and fitted the resulting ansatz to the correlation function. Neglecting contributions with even higher energy, the correlation function has the form

$$H(t; A, M) = A_1 h_+(t; M_0) + A_2 h_-(t; M_2) + A_3 h_+(t; M_3) + A_4 h_-(t; M_4) + \dots \quad (3a)$$

where

$$h_+(t, M) = e^{-Mt} + (-1)^{t-1} e^{-M(t-T)}, \quad (3b)$$

$$h_-(t, M) = -h_+(T-t, M). \quad (3c)$$

Each of the terms corresponds to one state and the sign factors included in the h_{\pm} originate from the staggered structure. The function in equation (3a) has 8 free parameter. Four masses and four prefactors. To stabilize the fit, we imposed priors on all but the ground state mass. These priors are motivated by measured excited states of the omega baryon [11] and quark model predictions [12] further motivated by [13, 14]. The central values of the priors were 2021 MeV, 2250 MeV, and 2400 MeV. The width were chosen to be 10 %, 10 %, and 15 %. No priors were applied to the prefactors. Since at early times, more than four states contribute to the correlation functions, we varied the time range of the fit. In addition, we fitted all ensembles at a given gauge coupling together by assuming that the quark mass dependencies of the mass parameters can be described by a linear function of the strange quark mass. The results from these fits combining multiple ensembles did not enter our main analysis but only served as a crosscheck.

As a complementary procedure, we also applied a GEVP based approach [10]. For that purpose we constructed the matrix

$$\mathcal{H}(t) = \begin{pmatrix} H_{t+0} & H_{t+1} & H_{t+2} & H_{t+3} \\ H_{t+1} & H_{t+2} & H_{t+3} & H_{t+4} \\ H_{t+2} & H_{t+3} & H_{t+4} & H_{t+5} \\ H_{t+3} & H_{t+4} & H_{t+5} & H_{t+6} \end{pmatrix}. \quad (4)$$

On such a matrix the well know staggered variational approach [16] can be applied. We solved the GEVP

$$\mathcal{H}(t_0) \vec{v}(t_a, t_b) = \lambda(t_a, t_b) \mathcal{H}(t_1) \vec{v}(t_a, t_b) \quad (5)$$

for two times t_0 and t_1 and then constructed a projected correlation function

$$C_i(t) = \vec{v}_i^\dagger(t_1, t_2) \mathcal{H}(t) v_i(t_1, t_2) \quad (6)$$

from the i -th generalized eigenvector \vec{v}_i . This projected correlation function is a linear combination of the time shifted correlation functions entering the matrix in equation (4). In contrast to the individual contributions in this matrix, the excited state contamination is however greatly reduced in $C(t)$. The effect of this procedure on a mock correlation function can be seen in figure 2 We

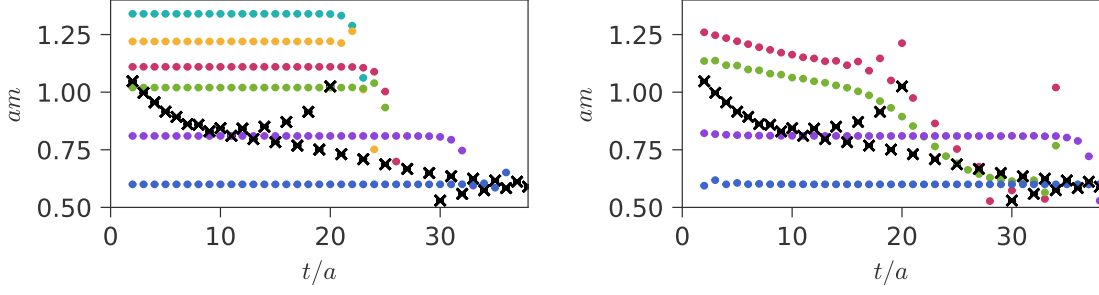


Figure 2: The effect of the GEVP based procedure as described in the main text on the effective mass. The black dots show the 2-lag effective mass of a mock correlation function and the colored dots show the same effective mass of the projected correlation function. The mock correlation function contains 6 states. For the left panel, a 6×6 matrix was employed whereas for the right panel, a 4×4 matrix was employed. The overlap with the ground state is improved significantly in both cases

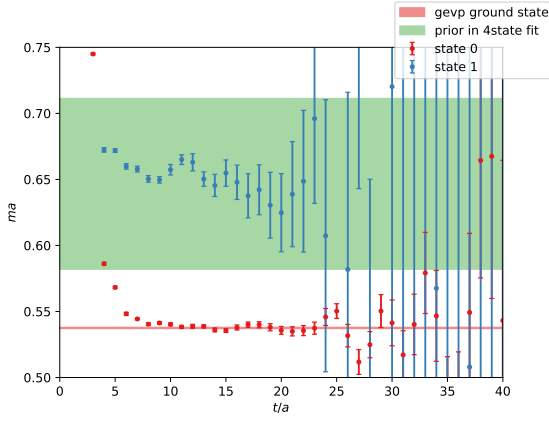


Figure 3: The projected correlation function for the groundstate and the first excited states on one ensemble. The dots show the effective masses of the projected correlation functions. The lower band indicates the mass extracted by a single exponential fit to the projected correlation function. The upper band is not obtained by the fit but indicates the width of the prior used in the alternative four state fit approach. As it can be seen, the first excited state mass as seen by the GEVP method is consistent with the prior.

used a standard one-state ansatz to extract the ground state mass from $C_0(t)$. The performance of the GEVP based method is shown for one ensemble in figure 3. There, also the effective mass of $C_1(t)$ is shown and compared to the prior for the first excited state in the four state fit approach. No priors are necessary for the GEVP based approach.

For our final determination, we employed three fits per ensemble: Two four state fits with different fit ranges and one combination of times for the GEVP base method. The combinations of fit ranges can be found in [1]. For each of the three procedures, a Kolmogorov-Smirnov test [15] was used to verify that the resulting χ^2 values were distributed as expected. For one value of the gauge coupling, the values of the omega masses determined with the described methods, are compared in figure 4.

2.2 QED contributions

The correlation function of a baryon operator in QCD+QED can be written to quadratic order in the valence and sea electrical charge and linear order in the strong isospin breaking as

$$\langle H \rangle_{\text{QCD+QED}} \approx \langle H \rangle_0 + \frac{\delta m}{m_l} \cdot \langle H \rangle'_m + \frac{e_v^2}{2} \cdot \langle H \rangle''_{20} + e_v e_s \cdot \langle C \rangle''_{11} + \frac{e_s^2}{2} \cdot \langle H \rangle''_{02}. \quad (7)$$

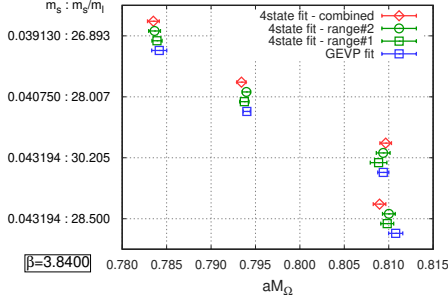


Figure 4: Comparison between the different determination of the omega mass on four ensemble with gauge coupling $\beta = 3.84$.

For more details of the formalism, see [1, 2, 17]. To determine the mass corrections, we apply the effective mass $\mathcal{M}[H]$ to H instead of the four state fits or GEVP based extractions because it features a closed form derivative with respect to the values of the correlation function H at different times which will be denoted as $\delta\mathcal{M}[H]/\delta H$. This allows to derive expression for the QED and strong isospin breaking correction to hadron masses. These corrections are

$$M_0 = \mathcal{M}[\langle H_0 \rangle_0] \quad (8a)$$

$$M''_{02} = \frac{\delta\mathcal{M}[H]}{\delta H} \Big|_{\langle H_0 \rangle_0} \langle H \rangle''_{02} = \frac{\delta\mathcal{M}[H]}{\delta H} \Big|_{\langle H_0 \rangle_0} \left\langle (H_0 - \langle H_0 \rangle_0) \frac{\text{dets}''_2}{\text{dets}_0} \right\rangle \quad (8b)$$

$$M''_{20} \approx \frac{1}{e_v^2} (\mathcal{M}[\frac{1}{2}\langle H_+ + H_- \rangle_0] - \mathcal{M}[\langle H_0 \rangle_0]) \quad (8c)$$

$$M''_{11} \approx \frac{\delta\mathcal{M}[H]}{\delta H} \Big|_{\langle H_+ + H_- \rangle_0} \left\langle \frac{H_+ - H_-}{2e_v} \frac{\text{dets}'_1}{\text{dets}_0} \right\rangle_0 \quad (8d)$$

$$M'_m \approx \frac{m_l}{\delta m} (\mathcal{M}[\langle H_{\delta m} \rangle_0] - \mathcal{M}[\langle H_0 \rangle_0]) \quad (8e)$$

where $\langle \dots \rangle_0$ is the QCD expectation value of \dots , H_0 is a combination of interpolating operators that can be used to measure the Omega mass in QCD, H_{\pm} are similar operators with positive and negative charges, $H_{\delta m}$ is a combination of interpolating operators with finite strong isospin breaking and dets_0 , dets'_1 , and dets''_2 are the appropriate products of quartic roots of fermion determinant and their first and second derivative with respect to the sea electric charge.

3. Global fits and the determination of w_0

For the determination of w_0 at the physical point and in the continuum, we employed a global fit. The approach discussed here is described in [1] under the name of Type 1 fit. For other global fits used in the determination of a_μ , especially to define the isospin splitting contributions, see that work. Let $Y = w_0 M_\Omega$. In general, such a dimensionless observable can be expanded around the physical point as

$$Y = A + BX_l + CX_s + DX_{\delta m} + Ee_v^2 + Fe_v e_s + Ge_s^2 \quad (9)$$

where

$$X_l = M_{\pi^0}^2/M_\Omega^2 - [M_{\pi^0}^2/M_\Omega^2]_* \quad , \quad X_s = M_{K^*}^2/M_\Omega^2 - [M_{K^*}^2/M_\Omega^2]_* \quad , \quad X_{\delta m} = \frac{(M_{K^0} - M_{K^+})^2}{M_\Omega^2} \quad (10)$$

with $M_{K_\chi}^2 = \frac{1}{2}(M_{K^0}^2 + M_{K^+}^2 - M_{\pi^+}^2)$ are suitable parametrizations of the light and strange quark mass deviations from the physical point and of the strong isospin splitting. The coefficients A, \dots, G are not assumed constant but to depend on the lattice spacing a , X_l , and X_s according to

$$A = A_0 + A_2 [a^2 \alpha_s^n (1/a)] + A_4 [a^2 \alpha_s^n (1/a)]^2 + A_6 [a^2 \alpha_s^n (1/a)]^3 \quad (11a)$$

$$B = B_0 + B_2 a^2 \quad (11b)$$

$$C = C_0 + C_2 a^2 \quad (11c)$$

$$D = D_0 + D_2 a^2 + D_4 a^4 + D_l X_l + D_s X_s \quad (11d)$$

$$E = E_0 + E_2 a^2 + E_4 a^4 + E_l X_l + E_s X_s \quad (11e)$$

$$F = F_0 + F_2 a^2 \quad (11f)$$

$$G = G_0 + G_2 a^2 \quad (11g)$$

where A_i, \dots, G_i are parameters to be determined by a fit and n determines the power of the α_s corrections to the continuum approach of the A term. For more details see [1].

Assuming $[\dots]_0$ to be the pure isospin symmetric QCD part of a given observable and $[\dots]'_m$, $[\dots]''_{20}$, $[\dots]''_{11}$, $[\dots]''_{02}$ being the first and second order derivatives with respect to the strong isospin breaking and the valence-valence, valence-sea, and sea-sea electric charges, equation (9) can be written as

$$[Y]_0 = [A + BX_l + CX_s]_0 \quad (12a)$$

$$[Y]'_m = [DX_{\delta m}]'_m \quad (12b)$$

$$[Y]''_{20} = [A + BX_l + CX_s + DX_{\delta m}]''_{20} + [E]_0 \quad (12c)$$

$$[Y]''_{11} = [A + BX_l + CX_s + DX_{\delta m}]''_{11} + [F]_0 \quad (12d)$$

$$[Y]''_{02} = [A + BX_l + CX_s + DX_{\delta m}]''_{02} + [G]_0 \quad (12e)$$

For the observable $Y = w_0 M_\Omega$, there is no strong isospin breaking component and hence equation (12b) is not needed. The other equations can be fitted to the lattice data in a simultaneous fit that takes into account the statistical correlations between the various quantities appearing in these equations.

Not all of the parameters listed above contribute to the determination of every observable. For this specific observable, we always enabled the parameters $A_0, A_2, C_0, E_0, F_0, G_0$ and set $n = 0$. To estimate the systematic uncertainty of our determination, we varied our global fitting form and the mass fits: One set of variations relates to changes in the fit ranges and methods of the mass fits for the omega mass and for the pseudoscalar meson masses. Another set of variation is introduced by imposing various cuts on the lattice spacing included in the fit. To estimate the systematic uncertainty introduced by our expansion we switched the fit parameters $A_4, B_0, C_2, E_2, E_l, E_s, F_2$, and G_2 on and off. We also varied the input mass of the omega baryon within the experimental uncertainty. All these variation lead to a large number of fits that we combine with the histogram method described in [1]. Some representative fits are shown in figure 5. We arrive at a result of

$$w_0 = 0.17236(29)(63)[70] \text{ fm}. \quad (13)$$

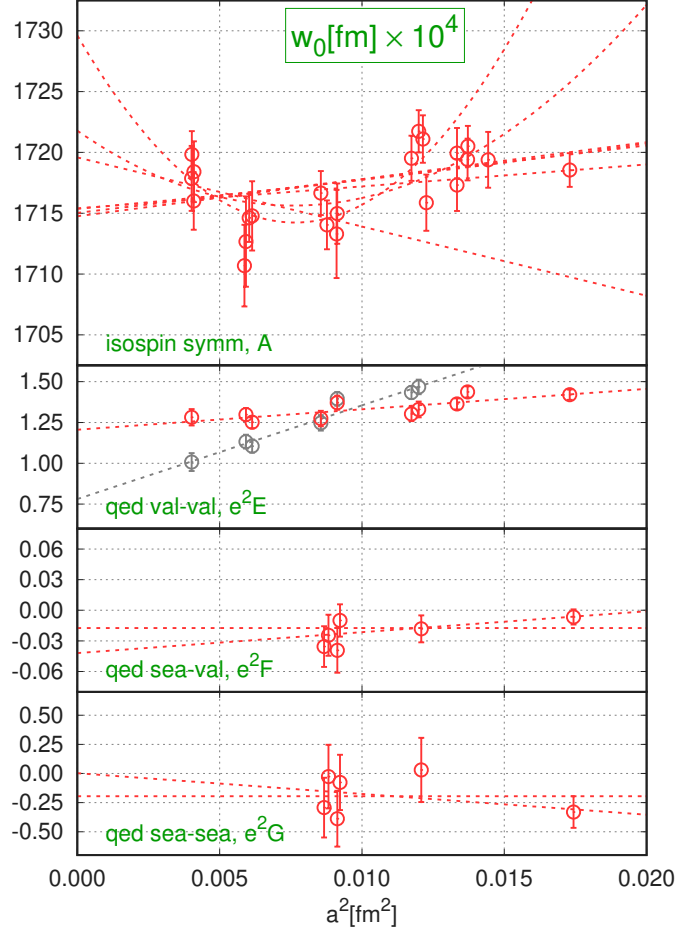


Figure 5: The continuum approach of the components in equations (12) and some representative global fits. The red points are the values of the components of Y measured on the various configurations. These points have already been extrapolated using the global fit with linear a^2 dependence to the physical point. For some fits these extrapolations yield significant different points. In that case, the points are shown in grey.

4. Conclusion

We have determined the w_0 scale in the continuum limit in full 2+1+1 flavour QCD+QED. This result can be used to precisely set the scale in subsequent lattice calculation. The method described here for the scale setting with the omega mass was also used in the high precision determination of the anomalous magnetic moment published in [1].

5. Acknowledgments

The computations were performed on JUQUEEN, JURECA, JUWELS and QPACE at Forschungszentrum Jülich, on SuperMUC and SuperMUC-NG at Leibniz Supercomputing Centre in München, on Hazel Hen and HAWK at the High Performance Computing Center in Stuttgart, on Turing and Jean Zay at CNRS' IDRIS, on Joliot-Curie at CEA's TGCC, on Marconi in Roma and

on GPU clusters in Wuppertal and Budapest. We thank the Gauss Centre for Supercomputing, PRACE and GENCI (grant 52275) for awarding us computer time on these machines. This project was partially funded by the DFG grant SFB/TR55, by the BMBF Grant No. 05P18PXFCA, by the Hungarian National Research, Development and Innovation Office grant KKP126769 and by the Excellence Initiative of Aix-Marseille University - A*MIDEX, a French “Investissements d’Avenir” program, through grants AMX-18-ACE-005, AMX-19-IET-008 - IPhU and ANR-11-LABX-0060.

References

- [1] S. Borsanyi et al., *Leading hadronic contribution to the muon magnetic moment from lattice QCD*, *Nature* **593** (2021) 51 [2002.12347].
- [2] B. Toth et al., *Muon $g-2$: BMW calculation of the hadronic vacuum polarization contribution*, *PoS LATTICE2021* (2022) 005.
- [3] S. Borsanyi et al., *High-precision scale setting in lattice QCD*, *JHEP* **09** (2012) 010 [1203.4469].
- [4] PARTICLE DATA GROUP collaboration, *Review of Particle Physics*, *PTEP* **2020** (2020) 083C01.
- [5] M.F.L. Golterman, *Staggered mesons*, *Nucl. Phys. B* **273** (1986) 663.
- [6] M.F.L. Golterman and J. Smit, *Lattice Baryons With Staggered Fermions*, *Nucl. Phys. B* **255** (1985) 328.
- [7] J.A. Bailey, *Staggered baryon operators with flavor $SU(3)$ quantum numbers*, *Phys. Rev. D* **75** (2007) 114505 [hep-lat/0611023].
- [8] S. Gusken, U. Low, K.H. Mutter, R. Sommer, A. Patel and K. Schilling, *Nonsinglet Axial Vector Couplings of the Baryon Octet in Lattice QCD*, *Phys. Lett. B* **227** (1989) 266.
- [9] C. Morningstar and M.J. Peardon, *Analytic smearing of $SU(3)$ link variables in lattice QCD*, *Phys. Rev. D* **69** (2004) 054501 [hep-lat/0311018].
- [10] C. Aubin and K. Orginos, *A new approach for Delta form factors*, *AIP Conf. Proc.* **1374** (2011) 621 [1010.0202].
- [11] BELLE collaboration, *Observation of an Excited Ω^- Baryon*, *Phys. Rev. Lett.* **121** (2018) 052003 [1805.09384].
- [12] S. Capstick and N. Isgur, *Baryons in a Relativized Quark Model with Chromodynamics*, *AIP Conf. Proc.* **132** (1985) 267.
- [13] A. Bazavov et al., *Additional Strange Hadrons from QCD Thermodynamics and Strangeness Freezeout in Heavy Ion Collisions*, *Phys. Rev. Lett.* **113** (2014) 072001 [1404.6511].
- [14] P. Alba et al., *Constraining the hadronic spectrum through QCD thermodynamics on the lattice*, *Phys. Rev. D* **96** (2017) 034517 [1702.01113].

- [15] S. Borsanyi et al., *Ab initio calculation of the neutron-proton mass difference*, *Science* **347** (2015) 1452 [[1406.4088](#)].
- [16] C. DeTar and S.-H. Lee, *Variational method with staggered fermions*, *Phys. Rev. D* **91** (2015) 034504 [[1411.4676](#)].
- [17] L. Parato et al., *QED and strong isospin corrections in the hadronic vacuum polarization contribution to the anomalous magnetic moment of the muon*, *PoS LATTICE2021* (2022) 358.